Early volatile depletion on planetesimals inferred from C–S systematics of iron meteorite parent bodies

Marc M. Hirschmann[a,1], Edwin A. Bergin[b], Geoff A. Blake[c], Fred J. Ciesla[d,e], and Jie Li[f]

[a]Department of Earth and Environmental Sciences, University of Minnesota, Minneapolis, MN 55455; [b]Department of Astronomy, University of Michigan, Ann Arbor, MI 48109; [c]Division of Geological and Planetary Sciences, California Institute of Technology, Pasadena, CA 91125; [d]Department of Geophysical Sciences, University of Chicago, Chicago, IL 60637; [e]Chicago Center for Cosmochemistry, University of Chicago, Chicago, IL 60637; and [f]Department of Earth and Environmental Sciences, University of Michigan, Ann Arbor, MI 48109

Contributed by Marc M. Hirschmann, February 24, 2021 (sent for review December 30, 2020; reviewed by Nancy L. Chabot and Richard J. Walker)

During the formation of terrestrial planets, volatile loss may occur through nebular processing, planetesimal differentiation, and planetary accretion. We investigate iron meteorites as an archive of volatile loss during planetesimal processing. The carbon contents of the parent bodies of magmatic iron meteorites are reconstructed by thermodynamic modeling. Calculated solid/molten alloy partitioning of C increases greatly with liquid S concentration, and inferred parent body C concentrations range from 0.0004 to 0.11 wt%. Parent bodies fall into two compositional clusters characterized by cores with medium and low C/S. Both of these require significant planetesimal degassing, as metamorphic devolatilization on chondrite-like precursors is insufficient to account for their C depletions. Planetesimal core formation models, ranging from closed-system extraction to degassing of a wholly molten body, show that significant open-system silicate melting and volatile loss are required to match medium and low C/S parent body core compositions. Greater depletion in C relative to S is the hallmark of silicate degassing, indicating that parent body core compositions record processes that affect composite silicate/iron planetesimals. Degassing of bare cores stripped of their silicate mantles would deplete S with negligible C loss and could not account for inferred parent body core compositions. Devolatilization during small-body differentiation is thus a key process in shaping the volatile inventory of terrestrial planets derived from planetesimals and planetary embryos.

iron meteorites | carbon | sulfur | planetary accretion | planetesimals

Major volatiles (H, C, N, and S) are inherently plentiful in the interstellar medium and abundant in primitive carbonaceous chondrites (CCs) (1, 2), but are scarce in terrestrial planets, which gained most of their mass from the inner parts of the solar nebula (3, 4). Formation of volatile-poor planets from a volatile-rich protoplanetary disk is a result of processes in the solar nebula, in accretion of precursor solids, and in interior differentiation. Addition of volatiles to nascent planets varies during accretion as protoplanetary systems become dynamically excited, contributing material originating from different heliocentric distances (3) and with different thermal histories. Much of this mass arrives in larger bodies (planetesimals or planetary embryos) that differentiated soon after formation (5). Key uncertainties include the nebular history of bulk materials that contributed volatiles to the rocky planets and how that affected their volatile cargos (6), and how planetesimal and planet formation influenced volatile distributions in accreted parent bodies.

Processes responsible for volatile deficits in terrestrial planets (7, 8) can occur either in the nebular, planetesimal, or planetary environment. Nebular volatile depletion could result from chemical interactions between nebular gas and dust, chondrule formation, or the accretion of thermally processed solids (9–11), perhaps owing to the hotter conditions prevailing closer to the protosun (4). Li et al. (6) argue that the comparatively small C inventory of the bulk Earth requires that nebular materials experienced significant early (<1 Ma) heating, before the "soot line" moved inward of 1 AU. Planetesimal processes involve loss to space during differentiation or processing of intermediate-sized bodies of tens to hundreds of kilometers in diameter (e.g., refs. 12 and 13). Planetary loss processes occur on large (thousands of kilometers in diameter) bodies (14, 15) in which gravity plays an appreciable role—including loss from impacts (16). The sum of these is an important determinant for whether terrestrial planets form with volatiles sufficient for habitability but not so great as to become ocean worlds (17) or greenhouse hothouses (18).

A key goal in the study of exoplanets and of young stellar systems is predicting environments and processes that could lead to habitable planets, including development of models that account for the distribution, acquisition, and loss of key volatile elements. Astronomical studies can reveal the architecture of other solar systems (19), the compositions of observable exoplanet atmospheres (ref. 20 and references therein), and the dust and volatile gas structure and composition of protoplanetary disks (ref. 21 and references therein), including interactions of the disk with gas- or ice-giant protoplanets. However, only limited astronomical observations can be made about conversion of disk materials (gas, dust, and pebbles) to planets in other solar systems. To understand this conversion, we must necessarily rely on planetesimals and their remnants (meteorites) as records of the processes that occurred. In this paper, we focus on volatile loss during planetesimal differentiation by examining evidence

Significance

Habitable rocky worlds require a supply of essential volatile elements (C, H, N, and S). These are plentiful in early solar systems but depleted during processes leading to planet formation. Here, evidence for loss during differentiation of small precursor bodies (planetesimals) is derived from iron meteorites, which are samples of planetesimal cores. Reconstruction of the C and S contents of planetesimal cores indicates severe C depletions compared to inferred original planetesimal compositions. Modeling of depletion processes shows that preferential loss of C compared to S is transferred to cores during differentiation. Iron meteorites preserve evidence of a key devolatilization stage in the formation of habitable planets and suggest pervasive carbon loss is likely associated with the birth of terrestrial worlds.

Author contributions: M.M.H. designed research; M.M.H. performed research; M.M.H., E.A.B., G.A.B., F.J.C., and J.L. analyzed data; and M.M.H., E.A.B., G.A.B., F.J.C., and J.L. wrote the paper.

Reviewers: N.L.C., Johns Hopkins University Applied Physics Laboratory; and R.J.W., University of Maryland.

The authors declare no competing interest.

[1]To whom correspondence may be addressed. Email: mmh@umn.edu.

This article contains supporting information online at https://www.pnas.org/lookup/suppl/doi:10.1073/pnas.2026779118/-/DCSupplemental.

Published March 22, 2021.

chiefly from iron meteorites. We note that ephemeral metal enrichments in white dwarf atmospheres confirm that differentiated planetesimals are common around other stars (22), and that our findings apply to how materials would have been processed during the assembly of other planetary systems.

In classic oligarchic growth models of planetary origin, planets and embryos grow from accretion of planetesimals with characteristic radii of tens to a few hundreds of kilometers (3). In pebble accretion models of terrestrial planet formation, the fraction of planetesimals in accreting material varies with time and protoplanetary mass (23), but still remains significant. Thus, for understanding volatile delivery to growing planets, an important question is whether the volatile inventory of accreting planetesimals (or larger objects) remained similar to that of primitive materials, typically taken to be comparable to chondritic meteorites, or had diminished significantly from prior differentiation.*

Achondritic meteorites are fragments of differentiated planetesimals and provide direct evidence of processes on small bodies.† Evidence for volatile loss on silicate achondritic parent bodies comes from elemental concentrations and from isotopes (24–27). However, the best-studied silicate achondritic suites, such as the eucrites and angrites, are igneous crustal rocks (28), and their compositions may not reflect average major volatile contents of their parent bodies. Volatile loss could have been locally enhanced by the igneous activity that produced the planetesimal crusts (29).

Iron meteorites offer an additional record of volatile processing in planetesimals. Many, known as "magmatic" irons, originated as metallic cores of planetesimals (30) and potentially record volatile depletions in their parent planetesimals at the time of alloy–silicate separation. Iron meteorites contain measurable amounts both major (S, C, N) and moderately volatile (Ge, Ga) elements and represent the cores of at least 50 parent bodies (31). Thus, known parent body cores are likely survivors from a population of planetesimals that were mostly incorporated into larger bodies and planets. Additionally, isotopic evidence links iron meteorites with both carbonaceous (CC) and noncarbonaceous (NC) chondrites (32), thereby correlating the differentiated planetesimals to their primitive chondritic heritage.

Here, we address the problem of planetesimal volatile loss by focusing on carbon and sulfur, two siderophile volatile elements that give important clues to the degassing history of metallic cores recorded iron meteorites and thereby their parent planetesimals.‡ We begin by examination of C–S systematics in different classes of chondrites. Although chondritic parent bodies formed later than most parent bodies of iron meteorites (33), they provide the best available guide to undifferentiated materials in the early solar system. Their isotopic kinships to iron meteorites (32) suggest that they derive from similar, although not necessarily identical, reservoirs, and so they provide a basis for comparison to those estimated for parent body cores. They also reveal devolatilization processes associated with planetesimal metamorphism. We then examine iron meteorite groups and reconstruct the compositions of their respective parent cores. Finally, we consider a spectrum of simple planetesimal core-formation scenarios and model the resulting C and S distributions. Comparison of these to reconstructed parent core C and S places new constraints on the magnitude of degassing occurring from planetesimal interiors.

S and C in Parent Cores and Other Cosmochemical Objects

To explore variations in C and S concentrations in planetesimals, we employ a log C/S versus log C plot (34) (Fig. 1). Processes leading to C enrichment or depletion without S variation produce diagonal trends on this graph, whereas independent S variations at constant C yield vertical trends.

C–S Variations in Primitive Planetesimals

Primitive planetesimals have not undergone differentiation to a metallic core and silicate mantle (±crust) and are represented in meteorite collections by chondrites and by primitive achondrites (28). Average C and S concentrations for chondrite groups (*SI Appendix*, Table S1) show coherent variation in log C/S versus log C along a diagonal trend that reflects significant depletions in C with more modest reductions in S concentration (Fig. 1*A*). CI, CM, CR, and TL carbonaceous chondrite groups comprise the C-rich end of the trend, while the strongly depleted CK carbonaceous and ordinary chondrites are the most C-poor. Intermediate concentrations are found in enstatite chondrites and CO, CV, and CB carbonaceous chondrites.

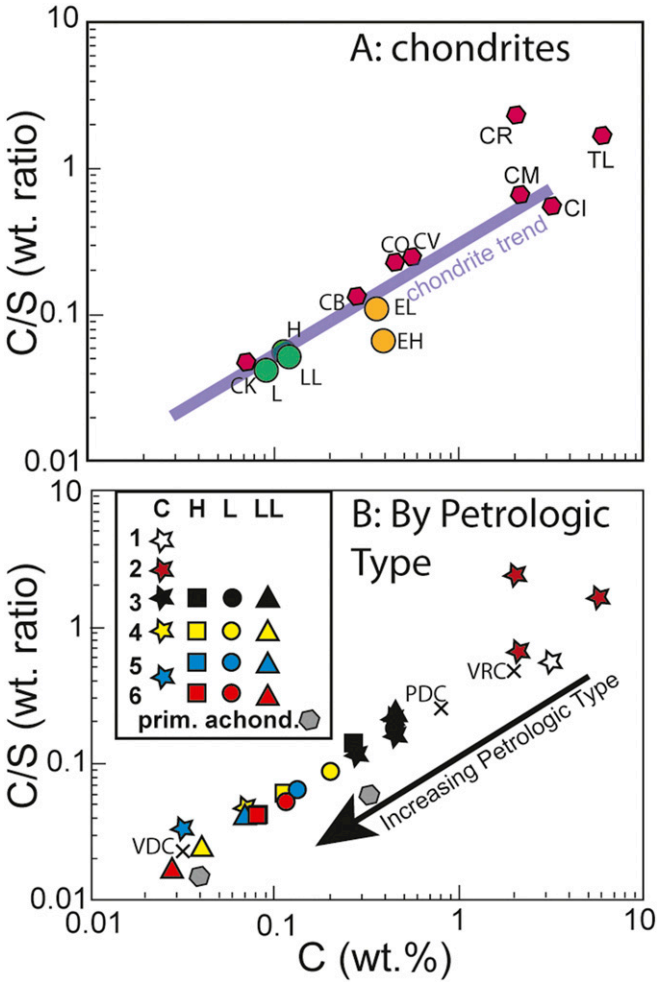

Fig. 1. C and S compositions of chondrite meteorite groups plotted as log C/S versus log C, following Hirschmann (34). (*A*) Average compositions of different chondrite groups; (*B*) average compositions of carbonaceous and ordinary chondrites, sorted by petrologic type, plus average compositions of primitive achondrite groups, acapulcoites, and winonaites. Data sources are given in *SI Appendix*, Table S1. Also shown are three model compositions used in calculations: VRC (volatile-rich chondrite), PDC (partially degassed chondrite), and VDC (volatile-depleted chondrite).

*Chondrites are meteorites that contain chondrules and are considered "primitive" in that they did not undergo enough thermal processing to produce phase separation, such as removal of molten metal or silicate.

†Achondrites are meteorites that have experienced sufficient thermal processing to destroy the chondrules that are characteristic of more primitive chondritic meteorites. These include both silicate achondrites as well as iron meteorites.

‡"Siderophile" elements are those that tend to concentrate in metallic alloys.

For the ordinary (H, L, LL) chondrite parent bodies, average concentrations taken from the compilation of Wasson and Kallemeyn (35) obscure considerable variations as a function of petrologic type, with higher types having lower C and C/S (Fig. 1*B*), which must reflect metamorphic processing on their parent planetesimals.[§] Variations seen between CC parent bodies reflect a similar dependence on petrologic type, but are evident mainly between groups from different parent bodies, which makes it difficult to separate the relative effects of nebular processes from those associated with planetesimal processes.

Primitive achondrites, which have experienced metamorphism sufficient to destroy textural evidence of chondrules, but not undergone wholesale silicate/alloy separation (28), are slightly displaced from the chondrite trend, with acapulcoites having compositions similar to chondrites of high petrologic type, but winonaites more similar to chondrites with intermediate petrologic type (e.g., H3, CV3, etc.).

C–S Variations in Parent Body Cores

Our goal is to use iron meteorite groups to estimate the composition of their molten parent cores prior to crystallization. Defining S and C concentrations in parent cores presents multiple challenges, owing partly to segregation of S and C in accessory phases and coarse heterogeneous textures that impede representative "average" bulk analyses (37) and partly to compositional variation within groups produced by extended fractional crystallization (38, 39). Furthermore, it is commonly inferred that selective destruction of S-rich differentiates causes S contents observed in irons to be biased to low concentrations not representative of bulk parent core compositions (40–42). For these reasons, estimates of S and C contents of parent body cores can conflict. Recognizing that each parent core must have unique mean S and C concentrations, we here adopt the strategy of considering multiple values where assessments diverge. This exercise will illustrate the extent to which the conclusions of this paper depend on the different estimates.

Analyzed bulk sulfur concentrations in iron meteorites generally range from 0 to 2 wt% (43), but many iron meteorite parent bodies are thought to be more S-rich (38–40, 42). Reconstruction of initial parent liquid S concentration is feasible for the magmatic iron meteorite groups, which show coherent fractional crystallization trends for trace elements (38, 39, 42, 44–48).

Because S has strong effects on liquid/solid alloy partition coefficients of trace elements (38, 40), bulk S contents of parent body cores can in theory be estimated from elemental modeling for those groups that show coherent differentiation trends. Such exercises indicate S-rich initial liquids ranging from 0.2 to 17 wt% (*SI Appendix*, Table S2), but resulting quantitative estimates show large differences depending on the methodology adopted. For example, Chabot (39) estimated 17 and 12 wt% S, respectively, in parental magma for the IIAB and IIIAB clans, whereas Wasson et al. (47) estimated 6 wt% S for IIAB and Wasson (38), 2 wt% for IIIAB parental liquids. The differences arise from different physical models for melt–solid segregation, with Wasson (38) and Wasson et al. (47) emphasizing the role of trapped liquid. We consider both sets of estimates (*SI Appendix*, Table S2).

Evaluation of C concentrations in iron meteorite groups is elaborated in *SI Appendix*. Low concentrations of C, ranging from 0.006 to 0.15 wt% (*SI Appendix*, Table S2), are a salient feature of the magmatic iron meteorites and are chiefly lower than even the most depleted chondrite groups (L 0.09 wt%; CK 0.07 wt%; *SI Appendix*, Table S1). Because C is siderophile (49), cores formed by closed-system segregation of molten metal from chondrite-like planetesimals would be expected to have greater C.

An important question is whether the low C concentrations inferred for parent body cores reflect the compositions of average solids crystallized from planetesimal cores, or if, similar to S, they are biased to low concentrations owing to systematic loss of samples formed from C-enriched liquid. However, unlike S, C has modest solubility in taenite (the FeNi alloy that crystallizes from melt, also known as austenite) (50). If magmatic iron meteorites represent cumulates, formation of C-rich liquids by fractional crystallization should be recorded by conjugate C enrichments in cumulates formed from more evolved liquids. However, within meteorite groups, C concentrations do not increase with Ni (51, 52), the chief major element indicator of differentiation. This observation led Goldstein et al. (37) to conclude that such C-rich liquids do not develop during fractional crystallization of planetesimal cores. They noted that the C–Ni systematics of iron groups contrast with correlations between P and Ni, which signify evolution of P-rich differentiates. The absence of C–Ni correlations suggests that estimates of C inferred from samples of an iron group may approximate original parent body core C concentrations, even if the particular meteorites crystallized from fractionated liquids.

A maximum estimate for the C contents of initial parent core liquids can be calculated by assuming that the igneous mineralogy of iron meteorites represents pure accumulations of crystallized alloy, without any trapped liquid (*SI Appendix*, Text). For the magmatic irons, the C content of parent liquids from which these cumulates precipitated can be found by matching the activity of C in solid Fe–Ni–C metal with that of a coexisting metal–sulfide–carbide liquid, using the liquid S contents inferred above. For this calculation, we employ a thermodynamic model of Fe–Ni–C taenite (50) and of Fe–C–S liquid (53). We neglect the effects of Ni on the liquid C activity liquid, which would diminish slightly the calculated liquid C content (54, 55). To the extent that some iron meteorites contain precipitated trapped liquid (38), rather than consisting of purely cumulus alloy, this calculation will overestimate the C of the calculated liquid for cases in which C behaves as an incompatible element, which applies when S contents are below ~10 wt%, and underestimate it for very S-rich liquids (see *SI Appendix* for further discussion).

For low S liquids, calculated C concentrations are modestly greater than inferred cumulate compositions, but for high S liquids, they are lower than the C of the corresponding solid meteorites (Fig. 2). The latter effect arises because S strongly enhances the C activity coefficient in Fe(Ni)–C–S liquids (53), as has been well documented in experimental studies of graphite solubility in sulfide liquids (55–58). Consequently, during planetesimal core crystallization, C behaves as a modestly incompatible element in liquids with <10 wt% S and a compatible element for more S-rich liquids (*SI Appendix*, Fig. S1). This contrasts with the common assumption that C is a strongly incompatible element during solidification of planetesimal cores (37, 59) and provides an explanation for why C enrichment is not recorded in the C–Ni systematics of individual parent bodies (37). Therefore, from both an empirical and theoretical perspective, the low C contents of magmatic iron meteorites are indicative of low C concentrations in parent cores, and not systematically biased by undersampling of putative C-rich late crystallized products.

The calculated C concentrations of parental liquids for each parent body are given in *SI Appendix*, Table S2 and illustrated in Fig. 2. We take these calculated liquid concentrations as approximations of the C contents of the core portions of the parent planetesimals (see *SI Appendix*, Text for further discussion). In the log C/S versus log C diagram, calculated parent cores fall chiefly into two different fields based on C/S ratio (Fig. 3), which we term "medium C/S" ($0.008 < C/S < 0.03$) and "low C/S" ($C/S < 0.006$), plus two higher C/S outliers. Note that the same

[§]Petrologic type is a measure of thermal and aqueous processing of the parent body, usually between types 1 and 6, with higher numeric values corresponding to greater temperatures (36).

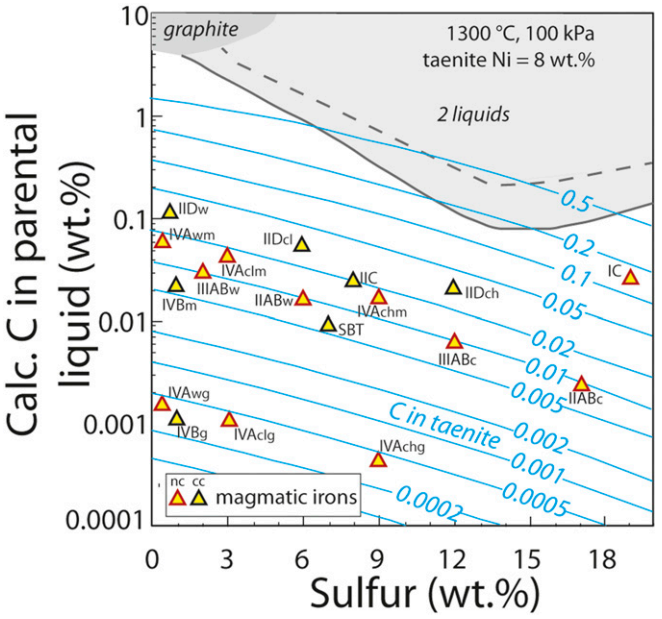

Fig. 2. C concentrations of planetesimal cores calculated from magmatic iron meteorite groups, using their inferred sulfur contents (*SI Appendix*, Table S2) and assuming that the C contents of iron meteorites (also *SI Appendix*, Table S2) represent pure cumulate taenite compositions (blue curves). Subscripts (key in *SI Appendix*, Table S2) denote different published estimates of S and/or C, as described in main text and *SI Appendix*, Text. From the assumed taenite composition, the activity of C is calculated from the thermodynamic model for Fe–Ni–C (50) at 100 kPa, 1,300 °C, assuming 8 wt% Ni. Higher temperatures would make C more compatible in the solid, resulting in lower calculated liquid C, and the calculations are not strongly dependent on the assumed Ni content for ±5 wt% (*SI Appendix*, Fig. S1). From this C activity, the liquid C concentration is calculated in Fe–C–S liquid with the specified S concentration from the model of Wang et al. (53). The fields of immiscible liquids and graphite saturation in the system Fe–C–S are shown for the 100-kPa liquidus surface from the thermodynamic model of Tafwidli and Kang (83). The dashed line is the estimated limit of the two-liquid field for 10 wt% Ni, based on experimental data (56, 84). No inferred core compositions are consistent with equilibrium with a second alloy liquid or graphite.

meteorite groups plot in different locations in this plot, depending on the source of estimated C and particularly S (*SI Appendix*, Table S2), the latter of which varies considerably depending on whether the methodology of Chabot or Wasson was employed. For example, the IVA irons are located in markedly different locations on the plot, depending on the S concentration estimate employed (Fig. 3 and *SI Appendix*, Table S2). However, nearly all such estimates result in core compositions with medium C/S or low C/S. The two high C/S outliers are considered further in *Discussion*.

Planetesimal Volatile Loss Processes

Processing on Planetesimals Similar to Chondrites. Heating of primitive bodies is accompanied by aqueous fluid transport and volatile loss (60, 61). The resulting effects on C and S can be gauged empirically from observed log C/S versus log C variations with petrologic type (Fig. 1*B* and *SI Appendix*, Table S1). Significant depletions in C with petrologic type are unsurprising, given that metamorphism, differentiation, and devolatilization, possibly including interior melting (60), occurred on chondrite parent bodies (62). S losses are evident for samples of higher petrologic type (e.g., the CK group). These metamorphic effects are consistent with observed decreases in highly volatile elements in ordinary chondrites with increasing petrologic type, without appreciable changes in moderately volatile concentrations (62).

The depletion of volatiles in chondritic bodies with increased textural equilibration must also have occurred during the early heating of planetesimals prior to separation of metal-rich melts that produced differentiated mantles and cores. This means that the immediate precursors to iron parent planetesimals were likely already partially devolatilized. The extent of devolatilization within a maturing planetesimal is not well understood, as it depends on location within bodies of varying radius, as well as the coevolution of thermal state, stresses, mineral reactions, and permeability (60, 61). In the following models of planetesimal differentiation, we consider three hypothetical precursor materials: a volatile-rich chondrite (VRC) similar to CI and CM groups, a volatile-depleted chondrite (VDC) similar in C and S concentrations to chondrites with petrologic types 5 or 6 or to acapulcoites, and partially depleted chondrite (PDC), intermediate between the VRC and VDC and somewhat more enriched than enstatite chondrites or chondrites of intermediate petrologic type (H3, CV3, etc.) (Fig. 1).

Processing on Differentiated Planetesimals. To explore the effects of planetesimal differentiation on C/S–C systematics of putative planetesimal cores, we model different scenarios, corresponding to progressively greater heating (Fig. 4). The simplest (Fig. 4*A1*) is segregation of a metallic core in a closed system by complete melting of the alloy but without appreciable melting of the silicate. A second case (Fig. 4*A2*) is formation of a planetesimal magma ocean beneath a solid impermeable outer shell (63, 64) in which molten alloy and silicate equilibrate without degassing to the surface. The third (Fig. 4*B*) and fourth (Fig. 4*C*) cases include formation of silicate melt in processes that allow surface degassing, with subsequent loss of this atmosphere. In the third

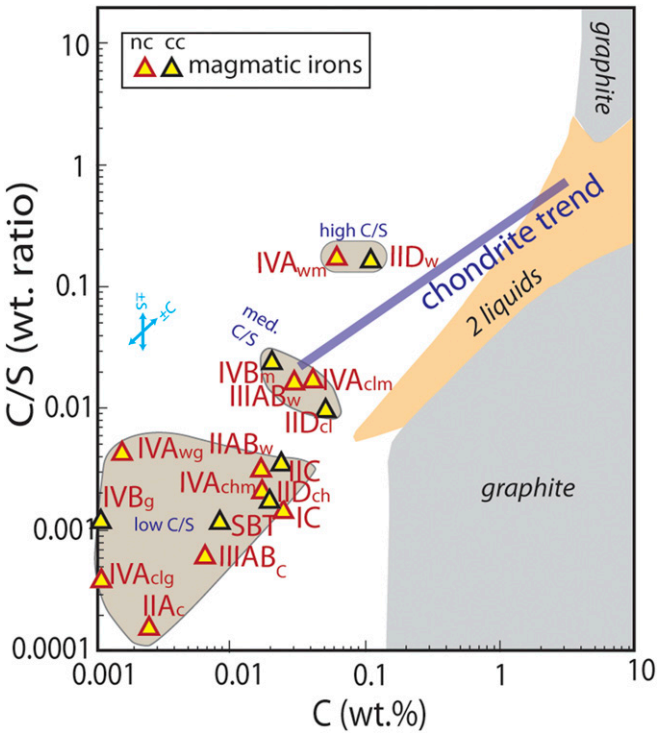

Fig. 3. C/S versus C compositions of planetesimal cores calculated for magmatic iron meteorite groups (*SI Appendix*, Table S2 and Fig. 2). Subscripts (key in *SI Appendix*, Table S2) are as described in caption to Fig. 2. The diagonal line shows the trend of chondritic compositions, from Fig. 1. Fields of immiscible liquids and graphite saturation in the system Fe–C–S are shown for the 100-kPa liquidus surface from the thermodynamic model of Tafwidli and Kang (83). The small blue arrows illustrate the effect of independent variation of C or S concentrations on the C/S versus C plot.

case (4B), degassing is limited and could be caused by volcanic eruptions or by impacts. Impacts can incite degassing by formation of limited surficial magma ponds (65) or by postimpact excavation of the interior (66, 67). Partial degassing is also expected in the multistage planetesimal core formation models proposed by Neumann et al. (68). In the fourth case (4C), degassing of the silicate portion of the planetesimal occurs owing to formation of an uncovered magma ocean (13). Formation of a wholly molten planetesimal is favored for large (>300-km) bodies formed within the first 0.5 Ma of solar system history owing to heating from ^{26}Al (13, 60). Fractionation of Mg and Si isotopes between silicate achondrite (HED, angrite) parent bodies relative to chondrites (24, 26) apparently requires significant high temperature degassing consistent with extensive near-surface magma (13).

For the case in which only alloy melts, C and S in the resulting core are controlled by the parent planetesimal bulk composition and the relative masses of silicate and metal. This assumes that no phases capable of storing appreciable C and S are retained in the silicate, but as discussed below and in *SI Appendix*, Text, some C may be retained in the silicate shell as graphite. Removal of all C and S to the core produces a liquid with the same C/S ratio as the bulk planetesimal, with C enhanced according to the inverse of the metal fraction in the planetesimal (Fig. 4*A*). For example, cores comprising 5 to 30% of the planetesimal mass with the PDC composition have 16 to 2.7 wt% C.

Models involving silicate melting require assumptions about relevant metal/silicate partition coefficients, which depend on oxygen fugacity and are detailed in *SI Appendix*, Table S3, and the degree of metal/silicate equilibration (69). In most scenarios, C is more siderophile than S (34), although in the case of segregation of S-rich (>18 wt% S) cores (applicable to VRC and PDC, but not VDC), the opposite relation holds (70) (*SI Appendix*, Table S3).

Cores from a sealed magma ocean are enriched in C and have C/S ratios similar to or greater than bulk planetesimal compositions, unless the cores are highly enriched in S, in which case the C/S ratios are lower than their source (Fig. 4*A*). Cores derived from planetesimals that have partially degassed during silicate melting are commensurately less enriched in C, with the specific C/S ratios controlled partly by the magnitude of C versus S outgassing (Fig. 4*B*). Cores formed from planetesimals that undergo wholesale melting have the lowest total C contents and also have markedly reduced C/S, owing to the much greater solubility of S in silicate melts relative to C (Fig. 4*C*).

Some of the calculated core compositions in Fig. 4, and particularly those derived from closed-system differentiation, plot within the fields of stability of two liquids or of graphite. Such liquids would partly crystallize or unmix, producing liquids at the boundaries of the graphite and two-liquid stability fields, respectively. Separation of S-rich liquids from graphite-saturated planetesimal mantles could leave behind C-enriched silicate residues with some similarities to ureilite achondrites (see *SI Appendix*, Text for further discussion).

Discussion

Parent Body Cores Produced from Degassing of Devolatilized Planetesimals. Modeled closed-system differentiation of planetesimals produces cores that are more enriched in C than those inferred than the medium and low C/S parent body cores (Fig. 4 *A* and *B*). For the less degassed VRC and PDC compositions, modeled cores have >20 times the C concentrations found in groups with medium and low C/S. For the much less C-rich VDC composition, modeled closed-system core compositions remain at least twice as C-rich. Prior to or coeval with core formation, planetesimals originating from material similar to chondrites and now represented by iron meteorites must have experienced considerable loss of highly volatile elements beyond that represented by even volatile-poor chondrites.

As noted above, model core compositions resulting from closed-system differentiation largely have compositions that are expected to unmix to C-rich and S-rich liquids, particular in the case of less degassed (VRC and PDC) bulk planetesimal compositions (Fig. 4*A*). For these, the S-rich conjugate liquids have >0.1 wt% C, and so are enriched in C compared to the parent body cores with medium C/S by factors of 2 to 10 (*SI Appendix*, Fig. S2). Origin of the medium C/S parent body cores simply by unmixing therefore seems unlikely. Once segregated to a core, a mechanism for secondary volatile loss would be required, but as argued below this additional process would have to be mediated by silicates, as devolatilization of bare iron cores would deplete S with little change in C and could not account for the observed C deficit.

The parent body cores with medium C/S can be reproduced if considerable silicate melting and degassing to the surface occurred prior to or during core formation, but only if the initial planetesimal had already been largely degassed, similar to the VDC composition (Fig. 4*B*). However, the low C/S parent bodies are so C-depleted that they require even more extensive degassing processes, as may have occurred in whole-planetesimal magma ocean scenarios (Fig. 4*C*).

Importance of Degassing of Silicates. A key inference is that evident planetesimal core volatile depletion occurred chiefly by loss from degassing of silicate or, prior to core formation, from silicate–metal portions of planetesimals. The metamorphic loss of volatiles that accounts for the chondrite trend (Fig. 1*B*) is owing to decomposition of accessory phases (mainly organics, sulfides) in a silicate-alloy matrix (62, 71, 72). The more advanced volatile loss and diminished C/S evident in the low C/S parent body cores is a hallmark of molten silicate degassing, owing to the greater solubility of S compared to C in such melts. Degassing of iron cores in the absence of silicate would have the opposite effect, as the vapor pressure of S above molten Fe–C–S alloy is orders of magnitude greater than that for C (Fig. 4*C* and *SI Appendix*, Text). Although some loss of volatiles from cores in the absence of their silicate mantles is not precluded, and has been inferred based on Pd–Ag isotopes for the IVA group (73), it would result in extensive loss of S without appreciable loss of C (Fig. 4*C* and *SI Appendix*, Text) and so cannot be the explanation for the low C/S of parent cores. We conclude that the parent planetesimals that produced extant iron meteorite groups were strongly depleted in carbon.

Effect of Conflicting Estimates of Core S Content and Significance of High C/S Outliers. The approach adopted here is to explore diverse and conflicting estimates of S and C for iron meteorites and for their planetesimals, and we find that the resulting inferences and conclusions do not depend on which sets of values are preferred. Irrespective of whether S-poor or S-rich parental metallic liquids for a particular iron group are accepted, nearly all calculated planetesimal cores fall either into the medium C/S or low C/S fields and both are populated by estimates that come from each methodology (Fig. 3). Thus, the conclusion that planetesimals parental to iron cores experienced significant degassing does not depend on establishing which methodology is more accurate.

Two apparent exceptions are high C/S outliers (IVA_W and IID_W in Fig. 3 and *SI Appendix*, Table S2) for which S contents of 0.4 and 0.7 wt% were calculated, respectively (45, 46), and which cannot be solely the products of the degassing processes modeled in Fig. 4. One interpretation is that the S concentrations of these are underestimated, perhaps because the melt/liquid partition coefficient of Ir, a key element in constraining liquid S content, was overestimated as compared to experimental results (39), resulting in underestimates of liquid S.

A second interpretation, offered to account for an inferred S-poor core for the otherwise volatile (Ge, Ga)-rich IID body, is two-stage disequilibrium core formation, resulting in a S-rich

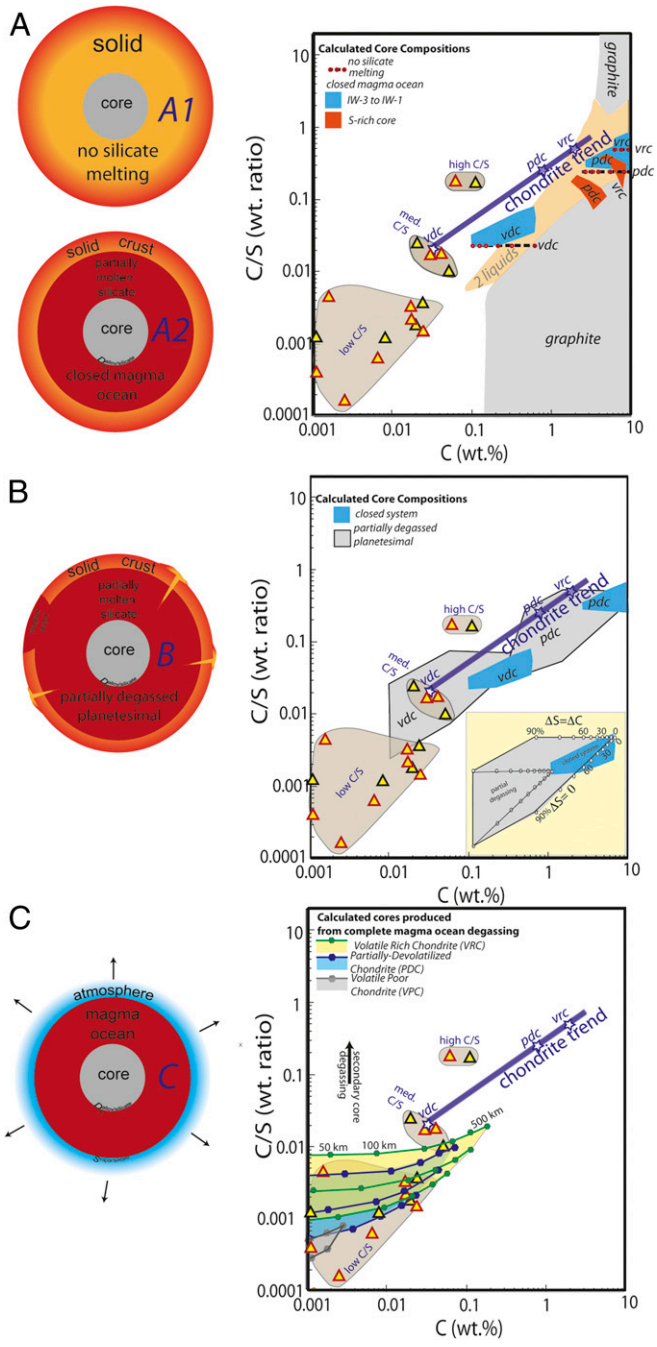

Fig. 4. Modeled core formation effects on planetesimals from chondritic precursors compared to inferred compositions of parent body cores (*SI Appendix*, Table S2 and Fig. 3). Three chondritic precursor compositions, VRC (volatile-rich chondrite), PDC (partially depleted chondrite), and VDC (volatile depleted chondrite) are used (*SI Appendix*, Table S1 and Fig. 1). For labels to individual iron meteorite groups, see Fig. 3. In *A*, two different core-forming processes are modeled. "No silicate melting" (cartoon *A1*) shows removal of alloy+C+S from each bulk composition planetesimals ranging from 5% (more C-rich cores) to 30% metal (less C-rich). "Closed magma ocean" (cartoon *A2*) shows removal of core alloy from a planetesimal with a solid carapace and interior magma ocean (63), with no degassing to the surface. Calculated core compositions are for planetesimals with 5 to 30% metal, partition coefficients given in *SI Appendix*, Table S3, and extent of metal–silicate equilibration ("*Q*" in *SI Appendix*, Text, Eq. **S1**) ranging from 50 to 100%. Partition coefficients are appropriate for core formation at oxygen fugacities of IW-3 to IW-1, as well as for formation of S-rich (>15 wt%) cores. The latter are not calculated for the VDC composition, which is too S-poor to generate S-rich cores. Some of the calculated core compositions plot within the stability fields of graphite or of two liquids (*SI Appendix*, Text). *B* models a "Partially degassed magma ocean" (calculated only for PDC and VDC compositions), which is similar to the "Closed magma ocean" calculations except that the molten silicate is assumed to have partially degassed to the planetesimal surface (cartoon *B*). *Inset* illustrates this, which is assumed to be loss of 0 to 90% of either the C ("Δ = 0", diagonal bound on each trend) or both the C and S ("ΔS = ΔC", horizontal bound), as further described in *SI Appendix*, Text. (*C*) Modeled cores produced by segregation from a planetesimal in which alloy was segregated from a magma ocean that had equilibrated with an atmosphere produced by whole-planetesimal degassing (cartoon *C*). Larger planetesimals produce atmospheres with greater partial pressures, thereby enhancing volatile retention in silicate and alloy portions. For each planetesimal bulk composition (VRC, PDC, and VDC), calculations are conducted for planetesimals with diameters of 500, 400, 300, 200, 100, 50, 20, and 10 km (with symbols in plot moving from C-rich to more C-poor as diameters diminish) and for partition coefficients appropriate for IW-3 (highest C/S for each bulk composition), IW-2, and IW-1 (lowest C/S). The vertical arrow shows the putative effect of secondary degassing of bare iron cores after differentiation and fragmentation of the parent meteorite. This results in extensive loss of S and negligible C loss, increasing the C/S ratio at constant C concentration.

outer core and S-poor inner core (46). However, this process alone could not account for the C concentrations of the IID body. Significant parent body outgassing of C prior to core segregation would also be required. Otherwise, the resulting S-poor inner core would be C-enriched, meaning it would plot to the C-rich side of the "chondrite trend" on Fig. 3.

A third possibility is outgassing of an exposed core from a planetesimal that had lost its silicate shell. As described in the previous section, this would deplete the core in S with negligible S loss, and thereby raise C/S, and such a process could be relevant to the IVA group based on Pd–Ag isotope systematics (73).

Significance for Volatile Delivery to Planets. Compared to precursors similar to chondrites, inferred planetesimal core compositions indicate that planetesimal differentiation was associated with significant volatile loss. The isotopic kinship between iron meteorites and chondrites, and in particular the observation that some of the metallic cores that are highly depleted in C (e.g., groups IIC and IVB) have CC parentage (32), makes clear that this depletion occurred on planetesimals, and was in addition to the devolatilization that occurs in primitive materials prior to planetesimal accretion (6). As documented in the modeling above, the volatile depletion processes, particularly those that resulted in low C/S, are characteristic of silicate degassing, which means that the inferred depletion affected the mantles of these planetesimals as well as their cores. The processes responsible for depletion of C, including metamorphic destruction of carbonaceous carriers in undifferentiated parent bodies and magmatic degassing into tenuous atmospheres, should also have pronounced effects on other highly volatile elements including nitrogen and hydrogen.

Isotopic evidence (33) and dynamical modeling (74) indicate that the parent body cores segregated from planetesimals and embryos born during early and efficient aggregation, whereas materials now preserved as chondrites formed late from remnant materials, possibly accreting as crustal veneers to earlier-formed differentiated planetesimals (33). Early formation of iron meteorite parent bodies and Mars (75), along with astronomical evidence for rapid drops in the observable mass of solids in disks (76), suggest that a large fraction of the raw materials for accreting planets was incorporated into planetesimals and embryos on ~100-ky timescales. Owing to ^{26}Al, such bodies would have reached high temperature, and thus undergone the processing described here. This effect should be more pronounced near 1 AU than in the asteroid belt, owing to more rapid planetesimal accretion timescales (77, 78). Therefore, if embryos and planets accreted chiefly from planetesimals, rather than from pebbles,

then the largely devolatilized planetesimals evidenced from parent body cores are likely better models for planetary feedstocks than chondrites. Lambrechts et al. (79) suggested that the flux of pebbles in the inner disk might lead to two modes of planet formation. Superearth-dominated systems form in the case of high pebble flux, whereas the low pebble flux regime favors formation of Mars-sized embryos, which in turn lead to giant-impact creation of terrestrial planets. The lack of superearths in our solar system suggests that this latter solution, with its greater role for planetesimals compared to pebbles, may be most relevant for the effects described here.

These considerations highlight that a significant fraction of the terrestrial planets were likely derived from differentiated objects that were unlike chondrites in their volatile cargos. This was particularly so for objects accreted during the early stages of planet formation and perhaps less prevalent for later-added materials arriving from high heliocentric distance (80, 81), although evidence from parent body cores shows that early-formed planetesimals derived from CCs also were degassed. This may have limited the supply of S and particularly C to cores of these planets. More generally, chondrites are probably poor guides for the sources of planetary volatiles, and the common modeling of planetesimals and embryos with chondritic compositions to account for the accretion of major volatiles to terrestrial planets (e.g., refs. 70, 80, and 81) is questionable. Recently, Piani et al. (82) suggested that about three oceans of H_2O could have been delivered by material similar to enstatite chondrites throughout its accretion, but this does not account for loss of H_2O during planetesimal or embryo differentiation, and so is likely an overestimate.

Conclusions

Loss from planetesimals is an important stage in the evolution from the volatile-rich solar nebula to volatile-poor, potentially habitable rocky planets. Iron meteorites provide a useful record of volatile processing and loss during planetesimal differentiation. Carbon concentrations in planetesimal cores represented by magmatic iron meteorite parent bodies can be estimated from the compositions of iron meteorites by assuming the latter are cumulates formed from the parent liquid and applying thermodynamic models for solid and liquid Fe-alloys and Fe–S–C liquid. Although the parent bodies are known to be variably enriched in S, they are all poor in C. This necessitates volatile carbon loss in the inner solar system via planetesimal and nebular processes.

Modeled closed-system core formation from chondrite-like planetesimals are significantly more enriched in C than inferred parent bodies of iron meteorites, highlighting that planetesimals experience open-system outgassing. Devolatilization comparable to that evident from high petrologic type chondrites is insufficient to account for the magnitude of carbon loss evident from the irons, indicating that silicate melting played a role in planetesimal evolution, either by surface magma oceans or more limited devolatilization processes, perhaps associated with impacts. Substantial C-depletion evident in parent body core compositions, but with significant remaining S, is consistent with volatile loss controlled by devolatilization and melting of silicates, but not with degassing of bare iron cores. Thus, the volatile-depleted character of parent body cores reflects processes that affected whole planetesimals. As the parent bodies of iron meteorites formed early in solar system history and likely represent survivors of a planetesimal population that was mostly consumed during planet formation, they are potentially good analogs for the compositions of planetesimals and embryos accreted to terrestrial planets. Less depleted chondritic bodies, which formed later and did not experience such significant devolatilization, are possibly less apt models for the building blocks of terrestrial planets. More globally, the process of terrestrial planet formation appears to be dominated by volatile carbon loss at all stages, making the journey of carbon-dominated interstellar precursors (C/Si > 1) to carbon-poor worlds inevitable.

Data Availability. All study data are included in the article and/or supporting information.

ACKNOWLEDGMENTS. We are grateful for the detailed and helpful reviews from Nancy Chabot and Rich Walker. This research comes from an interdisciplinary collaboration funded by the Integrated NSF Support Promoting Interdisciplinary Research and Education Program through Grant AST1344133. Additional funding has been provided by National Aeronautics and Space Administration Grants 80NSSC19K0959 (to M.M.H.), XRP NNX16AB48G (to G.A.B.), and XRP 80NSSC20K0259 (to E.A.B. and F.J.C.).

1. E. A. Bergin, G. A. Blake, F. Ciesla, M. M. Hirschmann, J. Li, Tracing the ingredients for a habitable earth from interstellar space through planet formation. *Proc. Natl. Acad. Sci. U.S.A.* **112**, 8965–8970 (2015).
2. K. Lodders, Solar system abundances and condensation temperatures of the elements. *Astrophys. J.* **591**, 1220–1247 (2003).
3. A. Morbidelli, J. I. Lunine, D. P. O'Brien, S. N. Raymond, K. J. Walsh, Building terrestrial planets. *Annu. Rev. Earth Planet. Sci.*, **40**, 251–275 (2012).
4. K. Mezger, M. Schonbachler, A. Bouvier, Accretion of the Earth-missing components? *Space Sci. Rev.* **216**, 27 (2020).
5. M. Wadhwa, G. Srinivasan, R. W. Carlson, "Time scales of planetesimal differentiation in the early solar system" in *Meteorites and the Early Solar System II*, D. S. Lauretta, H. Y. McSween, Eds. (University of Arizona Press, 2006), pp. 715–731.
6. J. Li, E. A. Bergin, G. A. Blake, F. J. Ciesla, M. M. Hirschmann, Earth's carbon deficit caused by early loss through irreversible sublimation. *Sci. Adv.*, in press.
7. A. N. Halliday, The origins of volatiles in the terrestrial planets. *Geochim. Cosmochim. Acta* **105**, 146–171 (2013).
8. B. Marty, The origins and concentrations of water, carbon, nitrogen and noble gases on Earth. *Earth Planet. Sci. Lett.* **313**, 56–66 (2012).
9. P. Cassen, Models for the fractionation of moderately volatile elements in the solar nebula. *Meteorit. Planet. Sci.* **31**, 793–806 (1996).
10. M. Humayun, P. Cassen, "Processes determining the volatile abundances of the meteorites and terrestrial planets" in *Origin of the Earth and Moon*, R. M. Canup, K. Righter, Eds. (University of Arizona Press, 2000), pp. 3–23.
11. C. Allegre, G. Manhes, E. Lewin, Chemical composition of the Earth and the volatility control on planetary genetics. *Earth Planet. Sci. Lett.* **185**, 49–69 (2001).
12. C. A. Norris, B. J. Wood, Earth's volatile contents established by melting and vaporization. *Nature* **549**, 507–510 (2017).
13. E. D. Young *et al.*, Near-equilibrium isotope fractionation during planetesimal evaporation. *Icarus* **323**, 1–15 (2019).
14. H. Genda, Y. Abe, Enhanced atmospheric loss on protoplanets at the giant impact phase in the presence of oceans. *Nature* **433**, 842–844 (2005).
15. J. C. Bond, D. S. Lauretta, D. P. O'Brien, Making the Earth: Combining dynamics and chemistry in the solar system. *Icarus* **205**, 321–337 (2010).
16. H. E. Schlichting, S. Mukhopadhyay, Atmosphere impact losses. *Space Sci. Rev.* **214**, 34 (2018).
17. A. Nakayama, T. Kodama, M. Ikoma, Y. Abe, Runaway climate cooling of ocean planets in the habitable zone: A consequence of seafloor weathering enhanced by melting of high-pressure ice. *Mon. Not. R. Astron. Soc.* **488**, 1580–1596 (2019).
18. B. J. Foley, A. J. Smye, Carbon cycling and habitability of Earth-sized stagnant lid planets. *Astrobiology* **18**, 873–896 (2018).
19. J. N. Winn, D. C. Fabrycky, The occurrence and architecture of exoplanetary systems. *Annu. Rev. Astron. Astrophys.*, **53**, 409–447 (2015).
20. N. Madhusudhan, Exoplanetary atmospheres: Key insights, challenges, and prospects. *Annu. Rev. Astron. Astrophys.*, , **57**, 617–663 (2019).
21. K. I. Oberg, E. A. Bergin, Astrochemistry and compositions of planetary systems. *Phys. Rep.* **893**, 1–48 (2021).
22. M. Jura, S. Xu, E. D. Young, ^{26}Al in the early solar system—not so unusual after all. *Astrophys. J. Lett.* **775**, L41 (2013).
23. A. Johansen, M. M. Low, P. Lacerda, M. Bizzarro, Growth of asteroids, planetary embryos, and Kuiper belt objects by chondrule accretion. *Sci. Adv.* **1**, e1500109 (2015).
24. E. A. Pringle, F. Moynier, P. S. Savage, J. Badro, J. A. Barrat, Silicon isotopes in angrites and volatile loss in planetesimals. *Proc. Natl. Acad. Sci. U.S.A.* **111**, 17029–17032 (2014).
25. C. Fitoussi, B. Bourdon, X. Y. Wang, The building blocks of Earth and Mars: A close genetic link. *Earth Planet. Sci. Lett.* **434**, 151–160 (2016).
26. R. C. Hin *et al.*, Magnesium isotope evidence that accretional vapour loss shapes planetary compositions. *Nature* **549**, 511–515 (2017).
27. A. R. Sarafian *et al.*, Early accretion of water and volatile elements to the inner solar system: Evidence from angrites. *Philos. Trans. A Math. Phys. Eng. Sci.* **375**, 20160209 (2017).
28. D. W. Mittlefehldt, "Achondrites" in *Treatise on Geochemistry*, H. D. Holland, K. K. Turekian, Eds. (Elsevier Pergamon, ed. 2, 2014), vol. 1, pp. 235–266.
29. D. W. Mittlefehldt, Volatile degassing of basaltic achondrite parent bodies - evidence from alkali elements and phosphorus. *Geochim. Cosmochim. Acta* **51**, 267–278 (1987).
30. J. T. Wasson, *Meteorites: Their Record of Early Solar- System History* (W. H. Freeman, 1985).

31. J. I. Goldstein, E. R. D. Scott, N. L. Chabot, Iron meteorites: Crystallization, thermal history, parent bodies, and origin. *Chemie Der Erde-Geochemistry* **69**, 293–325 (2009).
32. T. S. Kruijer, C. Burkhardt, G. Budde, T. Kleine, Age of Jupiter inferred from the distinct genetics and formation times of meteorites. *Proc. Natl. Acad. Sci. U.S.A.* **114**, 6712–6716 (2017).
33. T. Kleine, K. Mezger, H. Palme, E. Scherer, C. Munker, Early core formation in asteroids and late accretion of chondrite parent bodies: Evidence from Hf-182-W-182 in CAIs, metal-rich chondrites, and iron meteorites. *Geochim. Cosmochim. Acta* **69**, 5805–5818 (2005).
34. M. M. Hirschmann, Constraints on the early delivery and fractionation of Earth's major volatiles from C/H, C/N, and C/S ratios. *Am. Mineral.* **101**, 540–553 (2016).
35. J. T. Wasson, G. W. Kallemeyn, Compositions of chondrites. *Philos. Trans. R. Soc. Lond. A* **325**, 535–544 (1988).
36. W. R. Vanschmus, J. A. Wood, A chemical-petrological classification for chondritic meteorites. *Geochim. Cosmochim. Acta* **31**, 747–754 (1967).
37. J. I. Goldstein, G. R. Huss, E. R. D. Scott, Ion microprobe analyses of carbon in Fe-Ni metal in iron meteorites and mesosiderites. *Geochim. Cosmochim. Acta* **200**, 367–407 (2017).
38. J. T. Wasson, Trapped melt in IIIAB irons; solid/liquid elemental partitioning during the fractionation of the IIIAB magma. *Geochim. Cosmochim. Acta* **63**, 2875–2889 (1999).
39. N. L. Chabot, Sulfur contents of the parental metallic cores of magmatic iron meteorites. *Geochim. Cosmochim. Acta* **68**, 3607–3618 (2004).
40. A. Kracher, J. T. Wasson, The role of S in the evolution of the parental cores of the iron-meteorites. *Geochim. Cosmochim. Acta* **46**, 2419–2426 (1982).
41. E. R. D. Scott, A. Kracher, "Where are the troilite-rich iron meteorites from planetesimal cores?" in *51st Lunar and Planetary Science Conference* (Lunar and Planetary Institute, 2020), p. 1836.
42. P. Ni, N. L. Chabot, C. J. Ryan, A. Shahar, Heavy iron isotope composition of iron meteorites explained by core crystallization. *Nat. Geosci.* **13**, 611–615 (2020).
43. V. F. Buchwald, *Handbook of Iron Meteorites. Their History Distribution Composition and Structure* (University of California Press, 1975).
44. K. L. Rasmussen, D. J. Malvin, V. F. Buchwald, J. T. Wasson, Compositional trends and cooling rates of group-IVB iron-meteorites. *Geochim. Cosmochim. Acta* **48**, 805–813 (1984).
45. J. T. Wasson, J. W. Richardson, Fractionation trends among IVA iron meteorites: Contrasts with IIIAB trends. *Geochim. Cosmochim. Acta* **65**, 951–970 (2001).
46. J. T. Wasson, H. Huber, Compositional trends among IID irons; their possible formation from the P-rich lower magma in a two-layer core. *Geochim. Cosmochim. Acta* **70**, 6153–6167 (2006).
47. J. T. Wasson, H. Huber, D. J. Malvin, Formation of IIAB iron meteorites. *Geochim. Cosmochim. Acta* **71**, 760–781 (2007).
48. H. A. Tornabene, C. D. Hilton, K. R. Bermingham, R. D. Ash, R. J. Walker, Genetics, age and crystallization history of group IIC iron meteorites. *Geochim. Cosmochim. Acta* **288**, 36–50 (2020).
49. B. J. Wood, Carbon in the core. *Earth Planet. Sci. Lett.* **117**, 593–607 (1993).
50. T. Wada, H. Wada, J. F. Elliott, J. Chipman, Thermodynamics of fcc Fe-Ni-C and Ni-C alloys. *Metall. Trans. B* **2**, 2199–2208 (1971).
51. C. F. Lewis, C. B. Moore, Chemical analysis of thirty-eight iron meteorites. *Meteoritics* **30**, 195–205 (1971).
52. C. B. Moore, C. F. Lewis, D. Nava, "Superior analyses of iron meteorites" in *Meteorite Research*, P. M. Millman, Ed. (Springer, 1969), vol. 12, pp. 738–748.
53. C. Wang, J. Hirama, T. Nagasaka, B. Y. Shiro, Phase equilibria of the liquid Fe-C-S ternary system. *ISIJ Int.* **31**, 1292–1299 (1991).
54. A. Gabriel, P. Gustafson, I. Ansara, A thermodynamic evaluation of the C-Fe-Ni system. *Calphad* **11**, 203–218 (1987).
55. Z. Zhang, T. Qin, A. Pommier, M. M. Hirschmann, Carbon storage in Fe-Ni-S liquids in the deep upper mantle and its relation to diamond and Fe-Ni alloy precipitation. *Earth Planet. Sci. Lett.* **520**, 164–174 (2019).
56. Z. Zhang, P. Hastings, A. Von der Handt, M. M. Hirschmann, Experimental determination of carbon solubility in Fe-Ni-S melts. *Geochim. Cosmochim. Acta* **225**, 66–79 (2018).
57. Y. Li, R. Dasgupta, K. Tsuno, Carbon contents in reduced basalts at graphite saturation: Implications for the degassing of Mars, Mercury, and the Moon. *J. Geophys. Res. Planets* **122**, 1300–1320 (2017).
58. K. Tsuno, R. Dasgupta, Fe-Ni-Cu-C-S phase relations at high pressures and temperatures - The role of sulfur in carbon storage and diamond stability at mid- to deep-upper mantle. *Earth Planet. Sci. Lett.* **412**, 132–142 (2015).
59. A. Corgne, B. J. Wood, Y. W. Fei, C- and S-rich molten alloy immiscibility and core formation of planetesimals. *Geochim. Cosmochim. Acta* **72**, 2409–2416 (2008).
60. J. Castillo-Rogez, E. D. Young, "Origin and evolution of volatile-rich asteroids" in *Planetesimals, Early Differentiation and Consequences for Planets*, L. T. Elkins-Tanton, B. P. Weiss, Eds. (Cambridge University Press, 2017), pp. 92–114.
61. R. R. Fu, E. D. Young, R. C. Greenwood, L. T. Elkins-Tanton, "Silicate melting and volatile loss during differentiation in planetesimals" in *Planetesimals, Early Differentiation and Consequences for Planets*, L. T. Elkins-Tanton, B. P. Weiss, Eds. (Cambridge University Press, 2017), pp. 115–135.
62. L. Schaefer, B. Fegley, Outgassing of ordinary chondritic material and some of its implications for the chemistry of asteroids, planets, and satellites. *Icarus* **186**, 462–483 (2007).
63. L. T. Elkins-Tanton, Magma oceans in the inner solar system. *Annu. Rev. Earth Planet. Sci.*, **40**, 113–139 (2012).
64. T. Lichtenberg, G. J. Golabek, T. V. Gerya, M. R. Meyer, The effects of short-lived radionuclides and porosity on the early thermo-mechanical evolution of planetesimals. *Icarus* **274**, 350–365 (2016).
65. A. G. Tomkins, E. R. Mare, M. Raveggi, Fe-carbide and Fe-sulfide liquid immiscibility in IAB meteorite, Campo del Cielo: Implications for iron meteorite chemistry and planetesimal core compositions. *Geochim. Cosmochim. Acta* **117**, 80–98 (2013).
66. F. J. Ciesla, T. M. Davison, G. S. Collins, D. P. O'Brien, Thermal consequences of impacts in the early solar system. *Meteorit. Planet. Sci.* **48**, 2559–2576 (2013).
67. R. J. Lyons, T. J. Bowling, F. J. Ciesla, T. M. Davison, G. S. Collins, The effects of impacts on the cooling rates of iron meteorites. *Meteorit. Planet. Sci.* **54**, 1604–1618 (2019).
68. W. O. Neumann, T. S. Kruijer, D. Breuer, T. Kleine, Multi-stage core formation in planetesimals revealed by numerical modeling and hf-w chronometry of iron meteorites. *Meteorit. Planet. Sci.* **53**, 6209 (2018).
69. R. Deguen, M. Landeau, P. Olson, Turbulent metal-silicate mixing, fragmentation, and equilibration in magma oceans. *Earth Planet. Sci. Lett.* **391**, 274–287 (2014).
70. D. S. Grewal *et al*., The fate of nitrogen during core-mantle separation on Earth. *Geochim. Cosmochim. Acta* **251**, 87–115 (2019).
71. G. D. Cody *et al*., Organic thermometry for chondritic parent bodies. *Earth Planet. Sci. Lett.* **272**, 446–455 (2008).
72. Y. Kebukawa, S. Nakashima, M. E. Zolensky, Kinetics of organic matter degradation in the Murchison meteorite for the evaluation of parent-body temperature history. *Meteorit. Planet. Sci.* **45**, 99–113 (2010).
73. M. F. Horan, R. W. Carlson, J. Blichert-Toft, Pd-Ag chronology of volatile depletion, crystallization and shock in the Muonionalusta IVA iron meteorite and implications for its parent body. *Earth Planet. Sci. Lett.* **351**, 215–222 (2012).
74. S. J. Weidenschilling, Accretion of the asteroids: Implications for their thermal evolution. *Meteorit. Planet. Sci.* **54**, 1115–1132 (2019).
75. N. Dauphas, A. Pourmand, Hf-W-Th evidence for rapid growth of Mars and its status as a planetary embryo. *Nature* **473**, 489–492 (2011).
76. L. Tychoniec *et al*., Dust masses of young disks: Constraining the initial solid reservoir for planet formation. *Astron. Astrophys.* **640**, 15 (2020).
77. A. Ghosh, S. J. Weidenschilling, H. Y. McSween, A. Rubin, "Asteroidal heating and thermal stratification of the asteroid belt" in *Meteorites and the Early Solar System II*, D. S. Lauretta, H. Y. McSween, Eds. (University of Arizona Press, 2006), pp. 555–566.
78. R. E. Grimm, H. Y. McSween, Heliocentric zoning of the asteroid belt by Al-26 heating. *Science* **259**, 653–655 (1993).
79. M. Lambrechts *et al*., Formation of planetary systems by pebble accretion and migration How the radial pebble flux determines a terrestrial-planet or super-Earth growth mode. *Astron. Astrophys.* **627**, A83 (2019).
80. D. C. Rubie *et al*., Accretion and differentiation of the terrestrial planets with implications for the compositions of early-formed solar system bodies and accretion of water. *Icarus* **248**, 89–108 (2015).
81. D. P. O'Brien, K. J. Walsh, A. Morbidelli, S. N. Raymond, A. M. Mandell, Water delivery and giant impacts in the "Grand Tack" scenario. *Icarus* **239**, 74–84 (2014).
82. L. Piani *et al*., Earth's water may have been inherited from material similar to enstatite chondrite meteorites. *Science* **369**, 1110–1113 (2020).
83. F. Tafwidli, Y. B. Kang, Thermodynamic modeling of Fe-C-S ternary system. *ISIJ Int.* **57**, 782–790 (2017).
84. L. B. Tsymbulov, L. S. Tsemekhman, Solubility of carbon in sulfide melts of the system Fe-Ni-S. *Russ. J. Appl. Chem.* **74**, 925–929 (2001).